



Article

Reaction of 1-propanol with Ozone in Aqueous Media

Erika Reisz ^{1,*}, Agnes Tekle-Röttering ², Sergej Naumov ³, Winfried Schmidt ²
and Torsten C. Schmidt ⁴

¹ Faculty of Industrial Chemistry and Environmental Engineering,
University "Politehnica" of Timișoara Bulevardul Vasile Pârvan Nr. 6, 300223 Timișoara, Romania

² Westfälische Hochschule Gelsenkirchen, Neidenburger Strasse 43, 45877 Gelsenkirchen, Germany

³ Leibniz Institut für Oberflächenmodifizierung (IOM), Permoserstrasse 15, 04318 Leipzig, Germany

⁴ Universität "Duisburg-Essen, Instrumentelle Analytische Chemie und Zentrum für
Wasser- und Umweltforschung, Universitätsstrasse 5, 45117 Essen, Germany

* Correspondence: erika_reisz@yahoo.com or erika.reisz@upt.ro; Tel.: +40741121106

Received: 2 July 2019; Accepted: 22 August 2019; Published: 26 August 2019



Abstract: The main aim of this work is to substantiate the mechanism of 1-propanol oxidation by ozone in aqueous solution when the substrate is present in large excess. Further goals are assessment of the products, their formation yields as well as the kinetic parameters of the considered reaction. The reaction of ozone with 1-propanol in aqueous solution occurs via hydride transfer, H-abstraction and insertion. Of these three mechanisms, the largest share is for hydride transfer. This implies the extraction of an hydride ion from the activated C–H group by O₃ according to reaction: (C₂H₅)(H)(HO)C–H + O₃ → [(C₂H₅)(H)(HO)C⁺ + HO₃[−]]_{cage} → (C₂H₅)(H)(HO)C⁺ + HO₃[−]. The experimentally determined products and their overall formation yields with respect to ozone are: propionaldehyde—(60 ± 3)%, propionic acid—(27.4 ± 1.0)%, acetaldehyde—(4.9 ± 0.3)%, acetic acid—(0.3 ± 0.1)%, formaldehyde—(1.0 ± 0.1)%, formic acid—(4.6 ± 0.3)%, hydrogen peroxide—(11.1 ± 0.3)% and hydroxyl radical—(9.8 ± 0.3)%. The reaction of ozone with 1-propanol in aqueous media follows a second order kinetics with a reaction rate constant of (0.64 ± 0.02) M^{−1}·s^{−1} at pH = 7 and 23 °C. The dependence of the second order rate constant on temperature is described by the equation: $\ln k_{II} = (27.17 \pm 0.38) - (8180 \pm 120) \times T^{-1}$, which gives the activation energy, E_a = (68 ± 1) kJ mol^{−1} and pre-exponential factor, A = (6.3 ± 2.4) × 10¹¹ M^{−1} s^{−1}. The nature of products, their yields and the kinetic data can be used in water treatment. The fact that the hydride transfer is the main pathway in the 1-propanol/ozone system can probably be transferred on other systems in which the substrate is characterized by C–H active sites only.

Keywords: ozone; 1-propanol; hydride transfer; H-abstraction; insertion; kinetic data

1. Introduction

This paper is one of a series that tries to shed some light on ozone reactions with compounds characterised by C–H active sites only, compounds known as less reactive. In this context, the main aims are to elucidate the mechanism of 1-propanol reaction with ozone in aqueous media and to provide kinetic parameters that characterize this reaction (activation energy and pre-exponential factor).

To the best of our knowledge, there are only a few data in the literature on 1-propanol/ozone aqueous system and these refer mainly to the rate constants of 1-propanol reactions with oxidants such as O₃, HO•, and O•[−] at temperatures between 20 and 25 °C. This information is given in Table 1.

Table 1. Second order rate constants for the reactions of 1-propanol with various oxidising agents in aqueous media.

Oxidising Agent	K (M ⁻¹ s ⁻¹)	Working Conditions	References
O ₃	(0.37 ± 0.04)	pH = 2 t = (20 ± 0.5) °C	[1]
	(0.64 ± 0.02)	pH = 7 t = 23 °C	this work
HO•	2.8 × 10 ⁹	pH = 7	[2]
	1.5 × 10 ⁹	pH = 10.7	[3]
	1.5 × 10 ⁹	pH = 7	[3]
	2.7 × 10 ⁹		[4]
O• ⁻	1.5 × 10 ⁹	pH = 14	[4]

The reason why the mechanism of this reaction is of such great interest is the assumption that hydride transfer plays an important role when ozone attack occurs at a C–H bond. This pattern has already been reported for aqueous systems such as 2-propanol/ozone [5], *tert*-butanol/ozone and formate/ozone [6]. The elementary reaction that triggers this mechanism can be written as follows [5–7]:



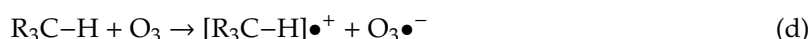
where R stands for hydrogen, organic or functional groups, identical or different.

The interpretation of experimental data for the system 2-propanol/ozone in organic media has led to the conclusion that ozone attack at C–H bond occurs via H-abstraction [8–10]:



The mechanism triggered by reaction (b) is not ruled out in aqueous media, but it plays a secondary role at least in the previously mentioned systems.

Other two possible interactions between ozone and substrate are insertion (reaction (c)) and electron transfer (reaction (d)):



In order to determine which of the four mentioned pathways is the most probable, Gibbs energies of the constituent reactions and overall formation yields of the products with respect to ozone were taken into consideration.

The results of this study, mainly the kinetic data and information about the nature and yields of products can also serve practical purposes, such as the treatment of wastewaters containing 1-propanol (1-propanol may be used as a solvent or as an ingredient of degreasing agents, antifreezes, disinfectants, inks, toners, dye solutions and also as a raw material for herbicides, insecticides, cosmetics and pharmaceuticals).

2. Results

2.1. Products

2.1.1. Hydroxyl Radical

As described in Materials and Methods Section, HO• formation yield with respect to ozone was determined indirectly by assessing formaldehyde formation yields with respect to ozone in the

1-propanol/O₃ system in the absence and presence of *tert*-butanol acting as a scavenger. In order to use this method, the reaction between substrate and O₃ should definitely prevail over that one between *tert*-butanol and O₃. In addition, the reaction of the substrate with HO• should be negligible with respect to that one between *tert*-butanol and HO•. Under our working conditions: [1-propanol] = 0.1 M and [*tert*-butanol] = 1 M, 98% of O₃ reacted with 1-propanol ($k(1\text{-propanol} + \text{O}_3) = (0.64 \pm 0.02) \text{ M}^{-1} \text{ s}^{-1}$ (this work) and $k(\text{tert-butanol} + \text{O}_3) = 1.1 \times 10^{-3} \text{ M}^{-1} \text{ s}^{-1}$ [6]) and 69% of HO• was scavenged by *tert*-butanol ($k(1\text{-propanol} + \text{HO}\bullet) = 2.7 \times 10^9 \text{ M}^{-1} \text{ s}^{-1}$ [4]) and $k(\text{tert-butanol} + \text{HO}\bullet) = 6 \times 10^8 \text{ M}^{-1} \text{ s}^{-1}$ [11,12]). Practically, HO• formation yield with respect to ozone was calculated with the following formula:

$$\eta(\text{HO}\bullet) = 2 \cdot \frac{(a - 0.31 \cdot b)}{0.69} \%$$

where: the factor 2 comes from the 50% formaldehyde formation yield with respect to HO• (more details are given in the Materials and Methods section), *a* and *b* are the formaldehyde formation yields with respect to ozone in the presence and absence of *tert*-butanol, 0.69 is the part of HO• that reacts with *tert*-butanol and 0.31 the part of HO• that reacts with 1-propanol in systems that contains both substrates next to ozone. The formaldehyde formation yields with respect to ozone, *a* and *b*, are derived from the slopes of the straight lines in the graphic representation of the formed formaldehyde concentration vs. the added ozone concentration, as shown in Figure 1. Under these circumstances HO• formation yield was $(9.8 \pm 0.3)\%$.

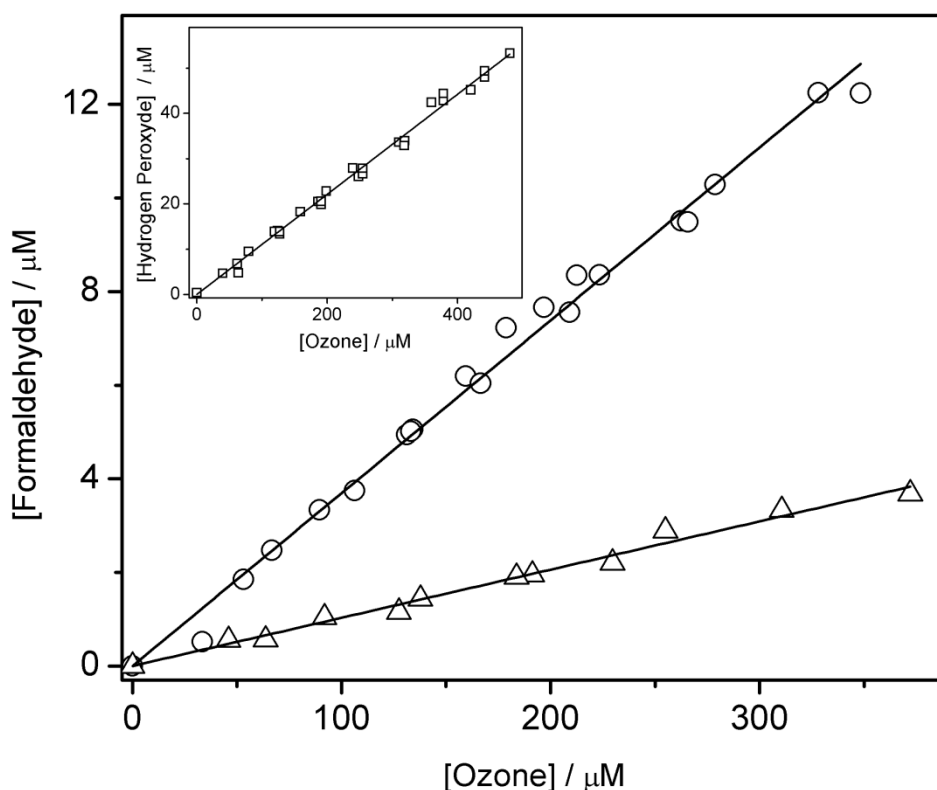


Figure 1. Main graph: determination of HO• formation yield with respect to ozone by using the formaldehyde formation yields in 1-propanol/ozone system in the absence (triangles) and presence of *tert*-butanol (circles) used as scavenger. Formaldehyde was determined spectrophotometrically with the Hantzsch method. [1-propanol] = 0.1 M, [*tert*-butanol] = 1 M. Inset: dependence of the formed hydrogen peroxide vs. added ozone concentrations. Hydrogen peroxide was determined spectrophotometrically by using Allen's method. [1-propanol] = 0.1 M.

This value indicates that the substrate is oxidized by both O₃ (direct reaction) and HO• (indirect reaction). Due to the fact that some of the products arise on both channels and that

one cannot make a clear distinction between the two contributions, the experimentally determined formation yields are called “overall formation yields”.

2.1.2. Aldehydes

As part of this category, propionaldehyde was formed by oxidation, while acetaldehyde and formaldehyde resulted from oxidative cleavage of 1-propanol.

Acetaldehyde and propionaldehyde were determined by means of high performance liquid chromatography (HPLC) and formaldehyde by spectrophotometric method. Details can be found in the Materials and Methods section.

The formation yield of propionaldehyde was $(60 \pm 3)\%$ and it was obtained from the plot of the formed propionaldehyde versus the added ozone concentrations, as shown in Figure 2.

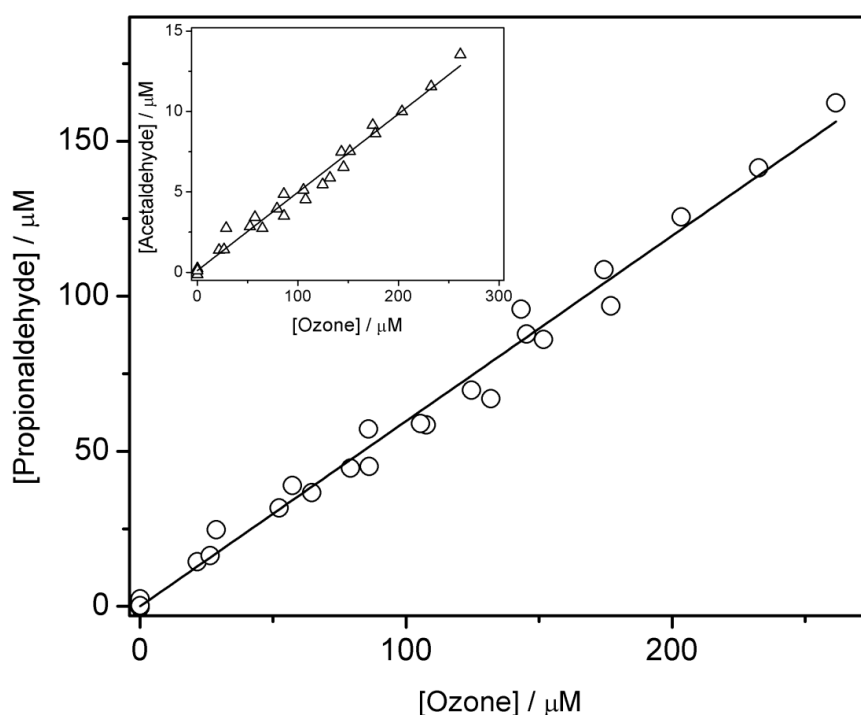


Figure 2. Main graph: dependence of the formed propionaldehyde versus added ozone concentrations. Inset: plot of the formed acetaldehyde versus added ozone concentrations. Propionaldehyde and acetaldehyde were determined as hydrazones by HPLC with optic detection. [1-propanol] = 0.1 M.

The formation yields for formaldehyde and acetaldehyde were one order of magnitude lower than the one for propionaldehyde. Thus, the formation yield of formaldehyde was $(1.0 \pm 0.1)\%$ and that one for acetaldehyde was $(4.9 \pm 0.3)\%$. These results were based on data from Figure 1 (for formaldehyde; triangles in the main graph) and the inset of Figure 2 (for acetaldehyde).

2.1.3. Acids

Of this category, propionic, acetic and formic acids formed within our system. Their concentrations were determined by way of ion chromatography (IC) as described in Materials and Methods section. The formation yields with respect to ozone were as follows $(27.4 \pm 1.0)\%$ —propionic acid, $(0.3 \pm 0.1)\%$ —acetic acid and $(4.6 \pm 0.3)\%$ —formic acid. These values were obtained based on data in Figure 3, which shows the dependence of the formed acid on opposing ozone concentrations.

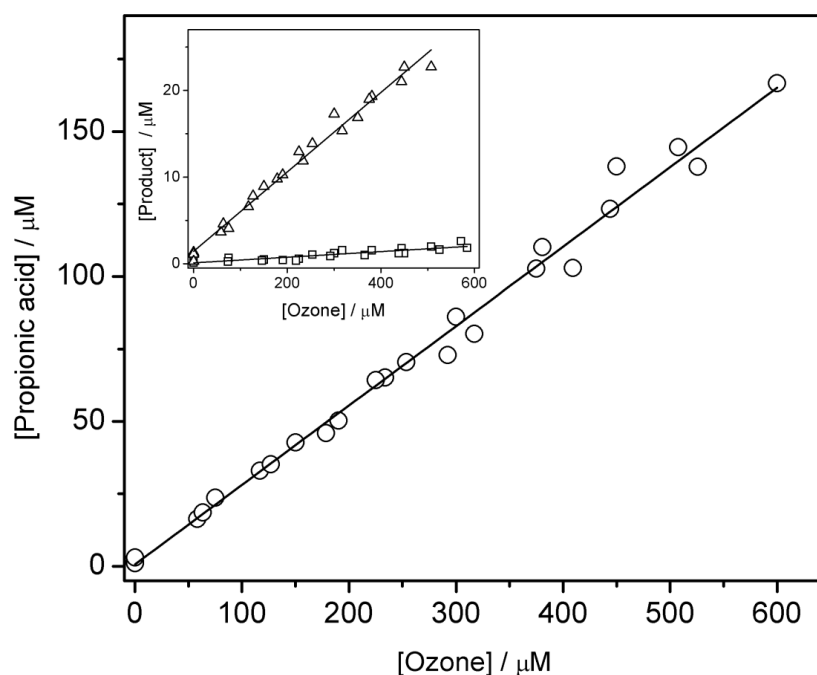


Figure 3. Main graph: dependence of the formed propionic acid versus added ozone concentrations. Inset: plots of the formed acetic and formic acids (squares and triangles, respectively) versus added ozone concentrations. Propionic, acetic and formic acids were determined by IC. [1-propanol] = 0.1 M.

2.1.4. Hydrogen Peroxide

The overall H_2O_2 formation yield with respect to ozone was determined from the plot of the formed H_2O_2 concentration versus added ozone, as shown in the inset of Figure 1. The resulted value was $(11.1 \pm 0.3)\%$. The H_2O_2 concentration was determined spectrophotometrically, as shown in Section 4.

2.1.5. Overview

Table 2 summarizes overall product formation yields in 1-propanol/ O_3 system. Firstly, these data show that the material balance is nearly closed, i.e., the sum of products formation yields with respect to O_3 is 93%. The remaining 7% is due to the practically unmeasurable low concentration of certain products (hydroxyacetone, hydroxyacetaldehyde and 1,2-propandiol), experimental errors, values used for molar absorption coefficients, etc. Secondly, one can notice that the sum of formation yields of compounds with one carbon atom (5.6%—resulted from 1.0% for formaldehyde and 4.6% for formic acid) equals that one corresponding to compounds with two carbon atoms (5.2%—obtained from 4.9% for acetaldehyde and 0.3% for acetic acid).

Table 2. Overview of the products formed in 1-propanol/ O_3 aqueous system and their overall formation yields with respect to O_3 .

Product	Propion-Aldehyde	Propionic Acid	Acet-Aldehyde	Acetic Acid	Form-Aldehyde	Formic Acid	Hydroxyl Radical	Hydrogen Peroxyde
Yield (%)	60 ± 3	27.4 ± 1.0	4.9 ± 0.3	0.3 ± 0.1	1.0 ± 0.1	4.6 ± 0.3	9.8 ± 0.3	11.1 ± 0.3

2.2. Kinetic Data

The first part of this section refers to determining the second order rate constant of the reaction between 1-propanol and ozone at 23 °C and comparing it with corresponding data in the literature and also with values reported for other alcohols.

The determination of the second order rate constant is based on graphic representation of the pseudo-first order rate constant, $k_{obs.}$, versus 1-propanol concentration, which practically remained unchanged throughout the reaction (Figure 4, main graph). To get the pseudo-first order rate constant, the variation of ozone absorbance at 260 nm was recorded as the reaction went on (Figure 4, upper inset), the natural logarithm of the ratio between current and initial absorbance was plotted versus time (Figure 4, lower inset) and finally the slope of the straight line was calculated ($\text{tg } \alpha = k_{obs.}$).

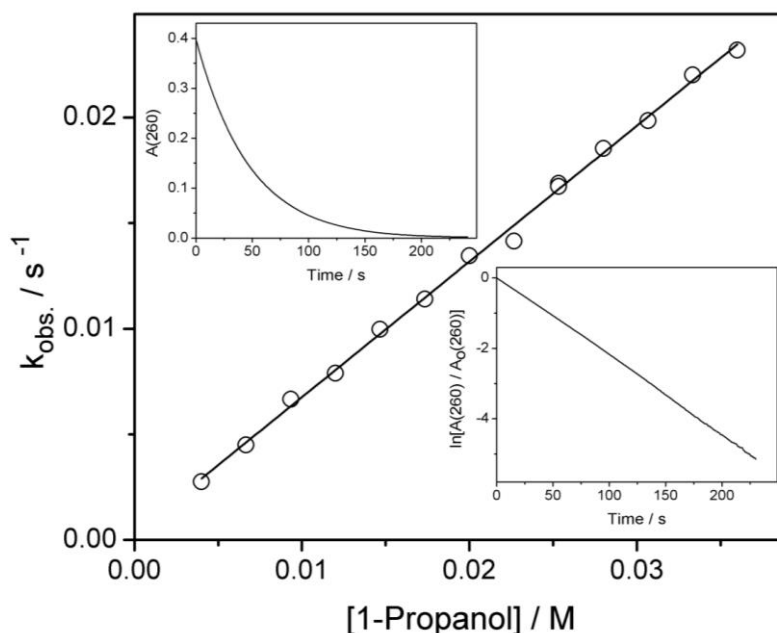


Figure 4. Main graph: Determination of the second order rate constant for the reaction of ozone with 1-propanol. Correlation of pseudo-first order rate constant (observed rate constant, $k_{obs.}$) with 1-propanol concentration at $t = 23\text{ }^{\circ}\text{C}$ and $\text{pH} = 7$ (as 1-propanol is in large excess with respect to ozone, the concentration of 1-propanol can be considered constant during reaction). Upper inset: exponential decrease of ozone concentration (measured as absorbance at 260 nm) versus time for $[1\text{-propanol}] = 36\text{ mM}$. Lower inset: the corresponding linear decrease of $\ln(A/A_0)$ versus time.

The resulting value for the second order rate constant at $\text{pH} = 7$ and $23\text{ }^{\circ}\text{C}$ is $(0.64 \pm 0.02)\text{ M}^{-1}\cdot\text{s}^{-1}$. Table 3 shows second order rate constants for reactions among O_3 and various alcohols.

By comparing the second order rate constants as determined by Hoigné and Bader at $20\text{ }^{\circ}\text{C}$ for primary alcohols [1], one can notice the increase of the reaction rate within series, from methanol to 1-octanol, following the increase of the electron repelling inductive effect as the number of carbon atoms within the organic chain increases. As expected, the rate constant also increases when the number of methyl groups that show electron repelling inductive effect increases. Table 3 highlights this influence for the switch from ethanol (one methyl group) to 2-propanol (two methyl groups).

The second part of this section deals with Arrhenius graphic representation in order to derive the second order rate constants at any given temperature within the considered range and also of the activation energy and pre-exponential factor. To get this information, the second order rate constants were determined for temperatures between 10 and $45\text{ }^{\circ}\text{C}$ and the natural logarithm of the second order rate constant was plotted against the inverse of absolute temperature, as in Figure 5. The explicit forms of dependencies $\ln k_{II} = f(T^{-1})$ and $k = f(T)$ are:

$$\ln k_{II} = (27.17 \pm 0.38) - (8180 \pm 120) \times T^{-1}$$

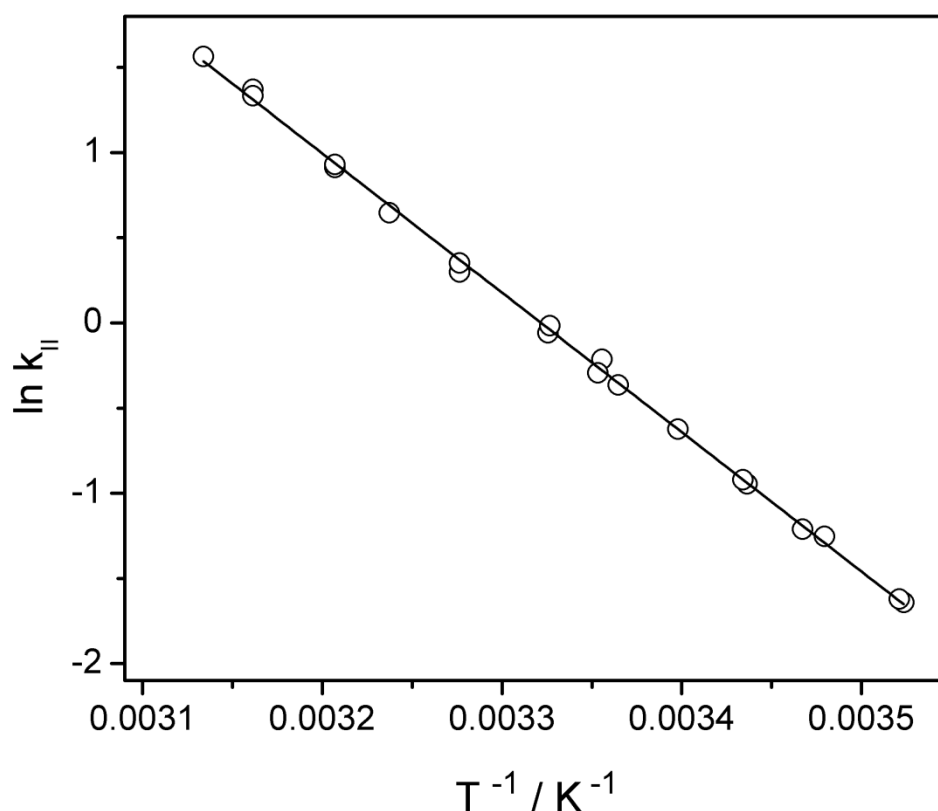
and

$$k_{II} = (6.3 \pm 2.4) \cdot 10^{11} \cdot e^{-\frac{(68 \pm 1) \cdot 10^3}{R \cdot T}}$$

Table 3. Second order rate constants for the reactions of O₃ with various alcohols (literature data).

C–H Bond Type	Alcohol	k _{II} (S + O ₃)	
		Value (M ⁻¹ s ⁻¹)	Reference
RH ₂ C–H	(H ₃ C) ₂ (HO)C H ₂ C–H (<i>tert</i> -Butanol)	1.1 × 10 ⁻³ 3 × 10 ⁻³	[6] * [1] **
	(HO)H ₂ C–H (Methanol)	2.4 × 10 ⁻²	[1] **
	(H ₃ C)(HO)HC–H (Ethanol)	(3.7 ± 0.4) × 10 ⁻¹	[1] **
R(HO)HC–H	(H ₅ C ₂)(HO)HC–H (1-Propanol)	(6.4 ± 0.2) × 10 ⁻¹ (3.7 ± 0.4) × 10 ⁻¹	this work * [1] **
	(H ₇ C ₃)(HO)HC–H (1-Butanol)	(5.8 ± 0.6) × 10 ⁻¹	[1] **
	(H ₁₅ C ₇)(HO)HC–H (1-Octanol)	<8 × 10 ⁻¹	[1] **
	(H ₃ C) ₂ (HO)C–H (2-Propanol)	(2.7 ± 0.1) (1.9 ± 0.2)	[5] * [1] **
R ₂ (HO)C–H	(H ₂ C) ₄ (HO)C–H (Cyclopentanol)	(2 ± 0.2)	[1] **

*—measured at 23 °C; **—measured at 20 °C.

**Figure 5.** Determination of the activation energy, E_a, and pre-exponential factor, A. Dependence between the natural logarithm of the second order rate constant and inverse of absolute temperature (Arrhenius plot).

These relations lead to (68 ± 1) kJ mol⁻¹ activation energy and (6.3 ± 2.4) × 10¹¹ M⁻¹ s⁻¹ pre-exponential factor.

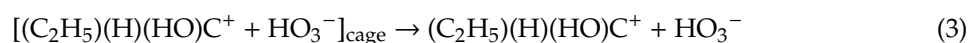
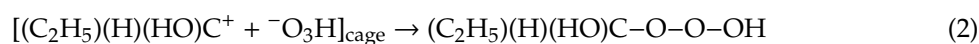
The second order rate constant at 20 °C and pH = 7 derived from the dependence $k = f(T)$ was $(4.7 \pm 0.2) \times 10^{-1} \text{ M}^{-1} \text{ s}^{-1}$ and it was in agreement with that reported by Hoigné and Bader of $(3.7 \pm 0.4) \times 10^{-1} \text{ M}^{-1} \text{ s}^{-1}$ at the same temperature and pH = 2 [1].

3. Discussion

3.1. Mechanism Initiated by the Direct Reaction of O_3 with 1-propanol

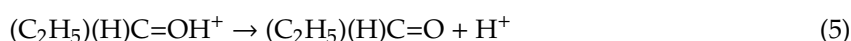
3.1.1. Hydride Transfer

In the first step, O_3 extracts a hydride ion from the activated C–H group thereby forming a carbocation and a hydrogen trioxide anion, HO_3^- ; this ion couple is kept together for some time within the solvent cage (reaction (1)). Further, these ions can recombine in the solvent cage forming α -hydroxyalkylhydrotrioxide (reaction (2), overall Gibbs energy for reactions (1) and (2), $\Delta G = -192 \text{ kJ mol}^{-1}$), or they can escape from the cage (reaction (3), overall Gibbs energy for reactions (1) and (3), $\Delta G = -167 \text{ kJ mol}^{-1}$).



One can notice that both successions of reactions ((1) plus (2) and (1) plus (3)) are highly exergonic and thus thermodynamically favoured. The fate of trioxide will be discussed as part of the paragraph that deals with the insertion mechanism.

The carbocation resulted following reaction (3) might rearrange by forming protonated propionaldehyde (reaction (4), $\Delta G = 0 \text{ kJ mol}^{-1}$), a species that is likely to lead to propionaldehyde by deprotonation (reaction (5), $\Delta G = -40 \text{ kJ mol}^{-1}$).



At the circumneutral pH of our experiments, hydrogen trioxide anion that resulted in reaction (3) will protonate forming hydrogen trioxide (reaction (6), $\text{pK}_a(\text{H}_2\text{O}_3) = (9.5 \pm 0.2)$ at 20 °C, $k_- = 9.2 \text{ s}^{-1}$, $k_+ = 10^{10} \text{ M}^{-1} \text{ s}^{-1}$ [13–15]), an unstable species in water, which decays by acid catalysis (reaction (7), $k = 6 \text{ M}^{-1} \text{ s}^{-1}$ [13–15], $\Delta G = -234 \text{ kJ mol}^{-1}$). The hydrogen trioxide anion itself undergoes decay to singlet oxygen and hydroxide ion (reaction (8), $\Delta G = -40 \text{ kJ mol}^{-1}$) [13].

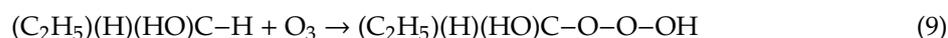


Given the reaction sequence initiated by a hydride ion transfer from 1-propanol to ozone (reactions (1), (3)–(8)), it follows that the sole stable product is propionaldehyde (except for oxygen). As the overall formation yield for propionaldehyde is $(60 \pm 3)\%$, it means that maximum $(60 \pm 3)\%$ of ozone has reacted with 1-propanol according to this mechanism (practically, by hydride transfer followed by ions escaping from the solvent cage).

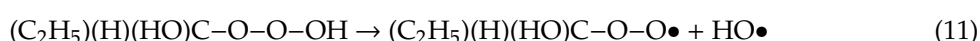
3.1.2. Insertion

This mechanism involves the intercalation of one O_3 molecule between carbon and hydrogen atoms of an activated C–H group, when α -hydroxyalkylhydrotrioxide forms (reaction (9),

$\Delta G = -192 \text{ kJ mol}^{-1}$). This trioxide might also form within the solvent cage via a hydride transfer mechanism (by recombination of the previously formed ion pair) and/or via H-abstraction (by recombination of the radical pair).



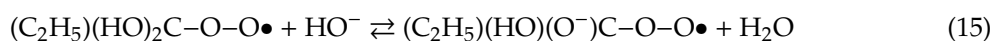
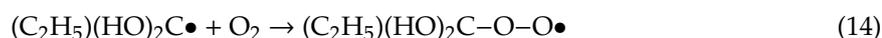
The resulted α -hydroxyalkylhydrotrioxide is likely to cleave to a secondary α -hydroxyalkyloxy radical and a hydroperoxy radical (reaction (10), $\Delta G = -14 \text{ kJ mol}^{-1}$) or to a secondary α -hydroxyalkylperoxy radical and a hydroxyl radical (reaction (11), $\Delta G = 46 \text{ kJ mol}^{-1}$). Both Gibbs energies of reactions and lengths of O–O bonds (1.442 Å for O–OOH and 1.426 Å for OO–OH) indicate that reaction (10) is favored over reaction (11).



The α -hydroxyalkyloxy radical might undergo 1,2-H shift (reaction (12), $\Delta G = -30 \text{ kJ mol}^{-1}$) or β -fragmentation (reaction (13), $\Delta G = -82 \text{ kJ mol}^{-1}$)



When O_2 is present, as in our system, it reacts with the dihydroxyalkyl radical formed in reaction (12), leading to a α -hydroxyalkylperoxy radical (reaction (14), $\Delta G = -101 \text{ kJ mol}^{-1}$), which itself is in equilibrium with the corresponding radical anion (reaction (15)).



The literature shows that as a general rule, α -hydroxyalkylperoxy radicals, $\text{R}_2(\text{HO})\text{C}-\text{O}-\text{O}\bullet$, eliminate $\text{HO}_2\bullet$ following a first order reaction that may be slow, the reaction rate constant depending on the nature of substituents [16–18]. The corresponding radical anions, $\text{R}_2(\text{O}^-)\text{C}-\text{O}-\text{O}\bullet$, eliminate $\text{O}_2\bullet^-$ very fast, following a second order process. Actually, this process consists of the equilibrium between the protonated and deprotonated species and $\text{O}_2\bullet^-$ elimination from deprotonated species, where the first step is the rate limiting one [7,19]. More details about $\text{HO}_2\bullet/\text{O}_2\bullet^-$ elimination are provided in Supplementary Materials.

Thus, the α -hydroxyalkylperoxy radical formed in reaction (14) is likely to eliminate $\text{HO}_2\bullet$ according to reaction (16) ($\Delta G = -98 \text{ kJ mol}^{-1}$) and the corresponding α -hydroxyalkylperoxy radical anion might eliminate $\text{O}_2\bullet^-$ as shown in reaction (17) ($\Delta G = -11 \text{ kJ mol}^{-1}$). Both reactions lead to propionic acid as a product.



Between $\text{HO}_2\bullet$ and $\text{O}_2\bullet^-$, as formed in reactions (16) and (17), one can write equilibrium (18) characterized by $\text{pK}_a = (4.8 \pm 0.1)$, which indicates that in our system ($\text{pH} \sim 7$), $\text{O}_2\bullet^-$ is the predominant species [20]. This could react with O_3 in excess, according to reaction (19), thus forming $\text{O}_3\bullet^-$, which is a precursor of $\text{HO}\bullet$. Given that in our experiments the substrate is in large excess ($[\text{2-propanol}] = 10^{-1} \text{ M}$,

$[O_3] \cong 5 \times 10^{-4} \text{ M}$), reaction (19) is less important, which means that insertion mechanism practically does not lead to the formation of $HO_2\bullet$.



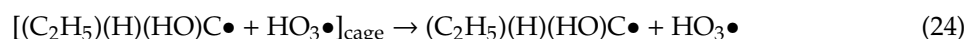
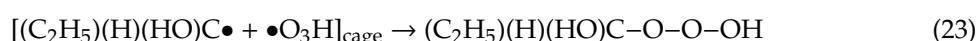
$HO_2\bullet/O_2\bullet^-$ are unstable species that can undergo bimolecular decay according to reactions (20) ($k = (8.3 \pm 0.7) \times 10^5 \text{ M}^{-1} \text{ s}^{-1}$) and (21) ($k = (9.7 \pm 0.6) \times 10^7 \text{ M}^{-1} \text{ s}^{-1}$) thereby forming H_2O_2/HO_2^- [20]. However, a bimolecular decay of $O_2\bullet^-$ does not take place to any significant extent [7].



According to reactions (9)–(21), it follows that the products resulted by the insertion mechanism are: propionic acid, formic acid, hydrogen peroxide, acetaldehyde and acetic acid (the last two compounds result following the oxidation of ethyl radical as a product of reaction (13)). The overall formation yields of these products are: $(27.4 \pm 1.0)\%$ —propionic acid, $(4.6 \pm 0.3)\%$ —formic acid, $(11.1 \pm 0.3)\%$ —hydrogen peroxide, $(4.9 \pm 0.3)\%$ —acetaldehyde and $(0.3 \pm 0.1)\%$ —acetic acid. From these formation yields it follows that trioxide is formed. However, this finding does not clarify whether trioxide forms following the insertion mechanism or by recombination of the ions formed by hydride transfer or of the radicals resulted from H-abstraction.

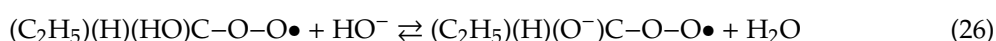
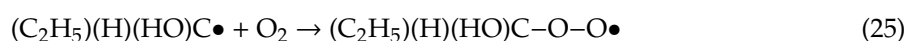
3.1.3. H-abstraction

This mechanism involves taking away one hydrogen atom from the activated C–H group as shown in reaction (22), when α -hydroxyalkyl and hydrogen trioxide radicals are likely formed. The radical pair is kept together for some time by the solvent cage where they can recombine to form trioxide (reaction (23), overall Gibbs energy for reactions (22) and (23), $\Delta G = -192 \text{ kJ mol}^{-1}$), or they can escape (reaction (24), overall Gibbs energy for reactions (22) and (24), $\Delta G = -19 \text{ kJ mol}^{-1}$). One can notice that both pathways are exergonic and thus thermodynamically possible; the formation of trioxide is thermodynamically favored given the one order of magnitude higher Gibbs energy (absolute value) than that for the formation of free radicals.



The fate of α -hydroxyalkyltrioxide has already been presented in the paragraph that deals with insertion mechanism (reactions (10)–(17)).

The α -hydroxyalkyl radical formed in reaction (24) might further reacts with oxygen that is in high concentration in our system, thereby most likely leading to α -hydroxyalkylperoxyl radical (reaction (25), $\Delta G = -95 \text{ kJ mol}^{-1}$). This species is in equilibrium with the corresponding radical anion (reaction (26)). Both the protonated and deprotonated species lead to propionaldehyde by elimination of $HO_2\bullet$ and $O_2\bullet^-$, respectively (reaction (27) characterized by $\Delta G = -27 \text{ kJ mol}^{-1}$ and reaction (28) with $\Delta G = -31 \text{ kJ mol}^{-1}$).





As has already been shown at the insertion mechanism:

- There is an acid-base equilibrium between $\text{HO}_2\bullet$ and $\text{O}_2\bullet^-$ (reaction (18));
- At the circumneutral pH within our system, $\text{O}_2\bullet^-$ is the predominant species ($\text{pK}_a(\text{HO}_2\bullet) = (4.8 \pm 0.1)$);
- Reaction between two $\text{HO}_2\bullet$ moles or between one $\text{HO}_2\bullet$ and one $\text{O}_2\bullet^-$ moles leads to the formation of H_2O_2 and HO_2^- , respectively (reactions (20) and (21));
- Given the large excess of substrate up against ozone within our system, reaction between $\text{O}_2\bullet^-$ and O_3 is not important and it follows that $\text{O}_3\bullet^-$ (as a precursor of $\text{HO}\bullet$) does not form practically via this pathway.

Due to the fact that α -hydroxyalkylperoxyl radical, formed in reaction (25), is a secondary peroxyl radical, it might also dimerize (reaction (29), $\Delta G = 94 \text{ kJ mol}^{-1}$):

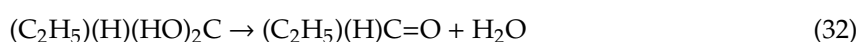
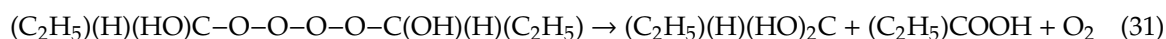


The formed tetroxide is actually a short lived intermediate that further might:

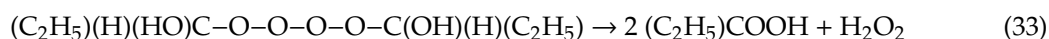
- Reform the α -hydroxyalkylperoxyl radical (reverse of reaction (29), $\Delta G = -94 \text{ kJ mol}^{-1}$);
- Eliminate O_2 , thus forming two α -hydroxyalkyloxyl radicals (reaction (30), $\Delta G = -180 \text{ kJ mol}^{-1}$) whose fate is described by the succession of reactions (12)–(17) at insertion mechanism;



- Decay via Russel reaction that involves a transition state with a six-membered ring (reaction (31), $\Delta G = -583 \text{ kJ mol}^{-1}$) [7,21]. Given that the diol formed in reaction (31) eliminates one water molecule intramolecularly according to reaction (32) ($\Delta G = -52 \text{ kJ mol}^{-1}$), the products are propionaldehyde, propionic acid, and oxygen in a 1:1:1 ratio;



- Decay via Bennett reaction that involves a transition state with two five-membered rings (reaction (33), $\Delta G = -752 \text{ kJ mol}^{-1}$) [7,17,22]. The products that form via this reaction are propionic acid and hydrogen peroxide in a ratio of 2:1.



The Supplementary Materials describes α -hydroxyalkylperoxyl radicals' transformation to products, according to Russel and Bennett mechanisms and the corresponding energy diagram. As already suggested, these processes occur in accordance with the following succession: Reactants \rightarrow First Transition State \rightarrow Intermediate (Tetroxide) \rightarrow Second Transition State \rightarrow Products.

Between $\text{HO}_3\bullet$ formed in reaction (24) and the corresponding anion, $\text{O}_3\bullet^-$, one can write the equilibrium (34). Given the $\text{pK}_a = -2$ of this reaction, it follows that $\text{HO}_3\bullet$ is a very strong acid and $\text{O}_3\bullet^-$ is the predominant species in our system [7,15,23–26]. The deprotonation occurs in the timescale of 10^{-12} s (reaction (34), $k_+ = 10^{12} \text{ s}^{-1}$) [23,24]. Under the same timescale, i.e., in competition with deprotonation, $\text{HO}_3\bullet$ decays to $\text{HO}\bullet$ and O_2 (reaction (35)) [7].



$O_3\bullet^-$ formed by deprotonation also acts as $HO\bullet$ precursor, but it decays in a larger timescale [6,24,25]. In the first step, $O_3\bullet^-$ cleaves to $O\bullet^-$ and O_2 (reaction (36), characterized by $K = 5.5 \times 10^{-7}$ M, $k_+ = (1.94 \pm 0.16) \times 10^3$ s $^{-1}$, $k_- = 3.5 \times 10^9$ M $^{-1}$ s $^{-1}$) [7,24,25,27] and then $O\bullet^-$ is protonated (reaction (37), $pK_a = (11.84 \pm 0.08)$) [27].



Hydroxyl radicals could undergo bimolecular decay thus leading to hydrogen peroxide (reaction (38), $k = 7.7 \times 10^9$ M $^{-1}$ s $^{-1}$) [28]. Due to the fact that the substrate is in very large concentration in our system ([1-propanol] = 0.1 M) it can be expected that $HO\bullet$ reacts mainly with the substrate and that reaction (38) is negligibly. The interaction of hydroxyl radical with the substrate is discussed at the paragraph no. 3.2. Mechanism initiated by the reaction of $HO\bullet$ with 1-propanol. It is also shown in Figure 7.

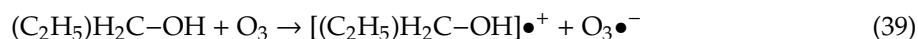


The products according to this mechanism are as follows: propionaldehyde, propionic acid, acetaldehyde, acetic acid, formic acid, hydrogen peroxide and hydroxyl radical. The overall formation yields, as experimentally determined, are as follows: propionaldehyde—(60 ± 3)%, propionic acid—(27.4 ± 1.0)%, acetaldehyde—(4.9 ± 0.3)%, acetic acid—(0.3 ± 0.1)%, formic acid—(4.6 ± 0.3)%, hydrogen peroxide—(11.1 ± 0.3)% and hydroxyl radical—(9.8 ± 0.3)%.

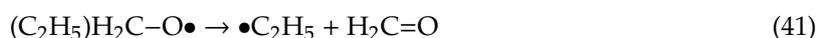
Due to the fact that $HO\bullet$ practically forms only via this mechanism, ozone consumption yield according to H-abstraction is expected to be equal to $HO\bullet$ formation yield, about 10%.

3.1.4. Electron Transfer

Ozone might also react with 1-propanol by withdrawing one electron when a radical cation and an ozonide anion are likely formed (reaction (39), $\Delta G = 100$ kJ mol $^{-1}$).



The radical cation might lose one proton (reaction (40), $\Delta G = -41$ kJ mol $^{-1}$) and the resulting alkyloxyl radical is likely to undergo β -fragmentation (reaction (41), $\Delta G = -19$ kJ mol $^{-1}$) and 1,2-H shift (reaction (42), $\Delta G = -48$ kJ mol $^{-1}$).



The hydroxyalkyl radical resulted following 1,2-H shift (reaction (42)), would further react according to the sequence formed from reactions (25)–(33).

The ozonide anion formed in reaction (39) would lead to $HO\bullet$ according to reactions (34)–(37).

Practically, the mechanism triggered by the electron transfer is ruled out, as suggested by the fact that the first step is strongly endergonic ($\Delta G = 100$ kJ mol $^{-1}$). One can notice that all products that could form via electron transfer also form through other mechanisms.

3.1.5. Overview

The possible pathways initiated by the direct reactions of ozone with 1-propanol are shown in Figure 6.

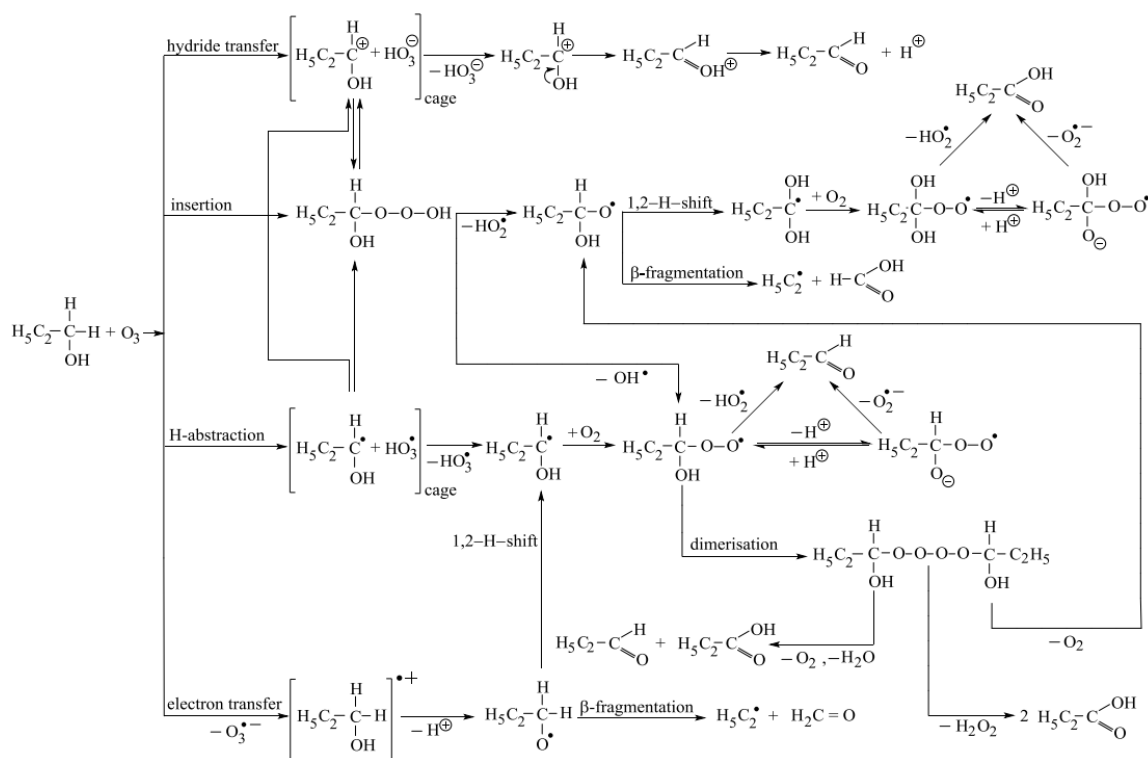


Figure 6. Pathways triggered by the direct reactions of ozone with 1-propanol.

Based on the above-mentioned discussion, it follows that of the four pathways by which ozone can react with 1-propanol directly, hydride transfer, insertion and H-abstraction are confirmed both by the thermodynamic data and quite high formation yields of the expected products. In the case of electron transfer, the highly positive value of Gibbs energy ($\Delta G = 100 \text{ kJ mol}^{-1}$) suggests that this reaction does not occur, which is also confirmed by the low overall formation yield of HO•, which actually forms via H-abstraction (for the first step, when HO₃• (HO• precursor) forms, Gibbs energy is $\Delta G = -19 \text{ kJ mol}^{-1}$).

By H-abstraction, 10% of the available ozone react and this percentage is given by HO• formation yield. The stable products as part of this pathway are propionaldehyde, propionic acid, acetaldehyde, acetic acid, formic acid and hydrogen peroxide. One can notice that although the overall formation yield with respect to ozone for propionic acid and propionaldehyde are $(27.4 \pm 1.0)\%$ and $(60 \pm 3)\%$, respectively, maximum 10% of the available ozone leads to the formation of these products by H-abstraction.

Hydride transfer mechanism leads only to propionaldehyde and due to the very high overall formation yield of this species, $(60 \pm 3)\%$, it means that, although it might also form by other pathways (H-abstraction and HO• attack at 1-propanol), hydride transfer is the main mechanism to a maximum 60% share of the studied mechanisms.

Insertion mechanism is likely to lead to propionic acid, acetic acid, acetaldehyde, formic acid and hydrogen peroxide. Given that the overall formation yield of propionic acid with respect to ozone is $(27.4 \pm 1.0)\%$, it follows that insertion is an important pathway, although this product can form also through H-abstraction and HO• attack at 1-propanol.

One must note that the three thermodynamically possible pathways are interconnected. Thus, the radical pair resulting from H-abstraction might undergo electron transfer, leading to the ion-pair resulting from hydride transfer ($\Delta G = -148 \text{ kJ mol}^{-1}$). Also the radical pair might recombine to form the trioxide ($\Delta G = -173 \text{ kJ mol}^{-1}$). In addition, an equilibrium is likely to be possible between the caged ion pair formed by hydride transfer and the trioxide formed after insertion. The reason for this is that the solvation energies of the ions might be underestimated by more than the difference between the

Gibbs energies of the two reactions ($\Delta G = -167 \text{ kJ mol}^{-1}$ for hydride transfer and $\Delta G = -192 \text{ kJ mol}^{-1}$ for insertion).

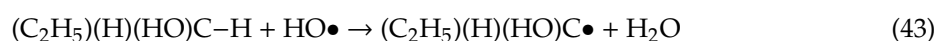
3.1.6. Comparison between 1-propanol/ozone and 2-propanol/ozone systems

The most important similarities or dissimilarities between the two aqueous systems are as follows:

- Carbonyl compounds with three carbon atoms formation yields with respect to ozone was very high for 2-propanol/ozone system (acetone formation yield was 87%) and decreased by 30% for the 1-propanol/ozone system (propionaldehyde formation yield was 60%). In the case of the 1-propanol/ozone system, propionic acid was also formed with a yield of 27%.
- Hydride transfer played a very important role for both systems, however the share of this mechanism was higher for the 2-propanol/ozone system (around 90% as opposed to maximum 60% for 1-propanol/ozone). The overall share of H-abstraction and insertion for 1-propanol/ozone system was higher or equal to 27% (propionic formation yield) and only a few percent for 2-propanol/ozone system.
- The second order rate constant of the reaction between 2-propanol and O_3 at 23 °C, $k_{II} = (2.7 \pm 0.1) \text{ M}^{-1} \text{ s}^{-1}$, was roughly four times higher than that between 1-propanol and O_3 , $k_{II} = (6.4 \pm 0.2) \times 10^{-1} \text{ M}^{-1} \text{ s}^{-1}$.
- Hydroxyl radicals formation yield was about four times higher for 1-propanol/ozone system, $(9.8 \pm 0.3)\%$, than that for 2-propanol/ozone, $(2.4 \pm 0.5)\%$. This information showed that the H-abstraction share was roughly four times higher in 1-propanol/ozone system than in 2-propanol/ozone (H-abstraction share was equal to $\text{HO}\bullet$ formation yield) and highlighted the increase of the importance of reactions between $\text{HO}\bullet$ and substrate for 1-propanol/ozone as against 2-propanol/ozone.

3.2. Mechanism Initiated by the Reaction of $\text{HO}\bullet$ with 1-propanol

Asmus and co-workers have found as part of their pulse radiolysis studies, that $\text{HO}\bullet$ attack on 1-propanol occurs at $\text{C}(\alpha)$ —53.4%, $\text{C}(\beta)$ —46% and OH —less than 0.5% [29]. The corresponding reactions are (43), (44) and (45), characterized by the following Gibbs energies: -123 kJ mol^{-1} , -107 kJ mol^{-1} and -76 kJ mol^{-1} , respectively. The attack of $\text{HO}\bullet$ on hydroxyl group will be neglected in the following discussion due to the low occurrence yield.



One can notice that the radical resulted in reaction (43) is the same as the one formed after H-abstraction (reactions (22) and (24)) and its fate can be followed in the paragraphs that deals with H-abstraction mechanism (reactions (25)–(33)) and insertion mechanism (reactions (12)–(17)). The resulting products (from the reaction of 1-propanol with both O_3 and $\text{HO}\bullet$) and the corresponding overall formation yields are: propionaldehyde— $(60 \pm 3)\%$, propionic acid— $(27.4 \pm 1.0)\%$, acetaldehyde— $(4.9 \pm 0.3)\%$, acetic acid— $(0.3 \pm 0.1)\%$, formic acid— $(4.6 \pm 0.3)\%$ and hydrogen peroxide— $(11.1 \pm 0.3)\%$.

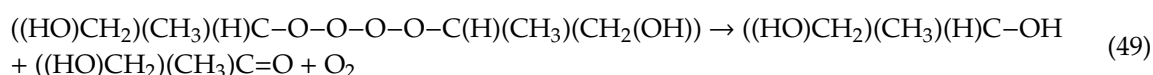
The radical formed in reaction (44) might add O_2 , which is in high concentration in our system, thereby leading to a peroxy radical (reaction (46), $\Delta G = -100 \text{ kJ mol}^{-1}$).



Given that this peroxy radical does not contain the hydroxyl group in α -position, it cannot eliminate $\text{HO}_2\bullet/\text{O}_2\bullet^-$ but, as a secondary peroxy radical, it might dimerise (reaction (47), $\Delta G = 85 \text{ kJ mol}^{-1}$).



The formed tetroxide is a short-lived intermediate that might: (a) reform the peroxy radical (reverse of reaction (47), $\Delta G = -85 \text{ kJ mol}^{-1}$), (b) eliminate oxygen (reaction (48), $\Delta G = -134 \text{ kJ mol}^{-1}$ and the Russel reaction (49), $\Delta G = -505 \text{ kJ mol}^{-1}$) and (c) eliminate H_2O_2 (Bennett reaction (50), $\Delta G = -627 \text{ kJ mol}^{-1}$).



The oxyl radical which occurred in reaction (48) is likely to decay by β -fragmentation (reaction (51), $\Delta G = -21 \text{ kJ mol}^{-1}$ and reaction (52), $\Delta G = -60 \text{ kJ mol}^{-1}$) and it might undergo 1,2-H shift (reaction (53), $\Delta G = -48 \text{ kJ mol}^{-1}$).



Reaction (53) is followed by an O_2 addition to the alkyl radical, when α -hydroxyalkylperoxy radical forms (reaction (54), $\Delta G = -69 \text{ kJ mol}^{-1}$). This is in equilibrium with the corresponding radical anion, according to reaction (55). Further, both protonated and deprotonated species form hydroxyacetone by eliminating $\text{HO}_2\bullet/\text{O}_2\bullet^-$ (reaction (56) characterised by $\Delta G = -46 \text{ kJ mol}^{-1}$ and reaction (57) with $\Delta G = -45 \text{ kJ mol}^{-1}$).



The products that might form via $\text{HO}\bullet$ attack on 1-propanol in β position are: 1,2-propanediol, hydroxyacetone, acetaldehyde, hydroxyacetaldehyde, formaldehyde, formic acid and hydrogen peroxide. Out of these products, only the overall formation yields with respect to ozone of a few were determined, as follows: acetaldehyde—(4.9 \pm 0.3)%, formaldehyde—(1.0 \pm 0.1)%, formic acid—(4.6 \pm 0.3)% and hydrogen peroxide—(11.1 \pm 0.3)%.

Due to the relatively low $\text{HO}\bullet$ formation yield with respect to ozone, (9.8 \pm 0.3)%, and taking into account that the yields of $\text{HO}\bullet$ attack at $\text{C}(\alpha)$ and $\text{C}(\beta)$ are 53.4% and 46%, respectively, it results that the products formation yields with respect to ozone might be a few percent at most for this pathway.

Figure 7 shows the succession of reactions triggered by the attack of $\text{HO}\bullet$ on 1-propanol.

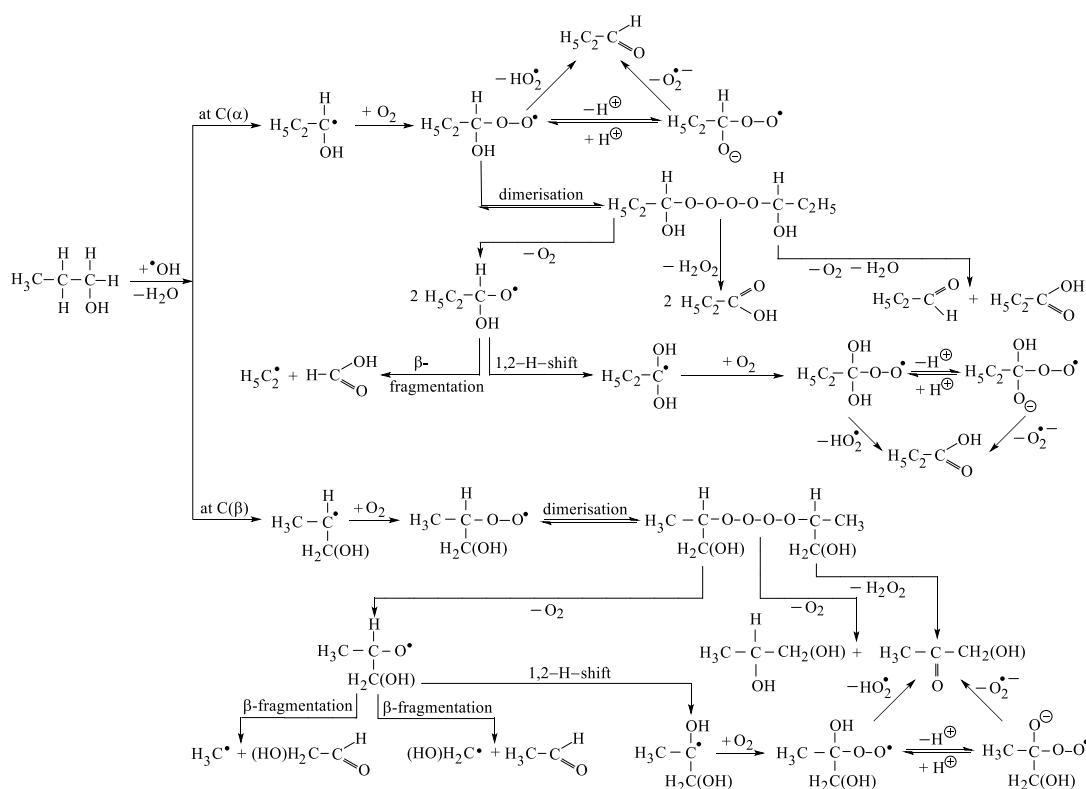


Figure 7. Pathways triggered by the attack of HO• on 1-propanol.

4. Materials and Methods

All chemicals were p.a. grade from: Merck (Merck Millipore, Darmstadt, Germany), Fluka (Fluka Chemie GmbH, Buchs, Switzerland), Fischer (Fischer Scientific GmbH, Schwerte, Germany), Alfa Aesar (Alfa Aesar, Karlsruhe, Germany) or Sigma Aldrich (Sigma Aldrich Chemie GmbH, München, Germany) and they were used without further purification. More information is given in Supplementary Materials.

Ozone solutions were prepared by bubbling ozone containing oxygen stream in type I Millipore water. Ozone containing gas was obtained by means of a Sander 300.5 ozone generator (Erwin Sander Elektroapparatebau GmbH, Uetze-Eltze, Germany) fed with oxygen 6.0 from Linde (Linde A.G., München, Germany). The type I water came from a Milli Q device (Merck Millipore, Darmstadt, Germany). Ozone and 1-propanol solutions were mixed in various proportions. The concentration of ozone in both freshly prepared ozone solutions and in those that resulted after mixing with 1-propanol was determined spectrophotometrically at 260 nm by using $\epsilon(260) = 3200 \text{ M}^{-1} \text{ cm}^{-1}$ [7]. All spectrophotometric measurements were carried out with a Shimadzu UV 1800 device (Shimadzu Europa GmbH, Duisburg, Germany).

Kinetic studies were carried out in the presence of large 1-propanol excess with respect to ozone to secure half-life times of minutes. Under these circumstances, the ozone decay via HO• was negligible. More details are provided in Supplementary Materials. Practically, 1 mL ozone solution (about 15 °C) was added to 14 mL 1-propanol solution, previously brought to the required temperature, in a 5 cm thermostated quartz cuvette. The temperature of the solution was measured with a dipped thermocouple before ozone addition and after completion of the reaction. The difference between the two temperatures did not exceed 0.4 °C. Ozone decay was followed spectrophotometrically by using the time-drive mode.

The formed acids (formic, acetic and propionic acids) were quantified by means of IC with conductometric detection. The analyses were carried out by using a Metrohm 883 Basic IC plus device (Metrohm, Herisau, Switzerland) equipped with a Metrosep Organic Acids 250/7.8 column

(Metrohm, Herisau, Switzerland). The eluent was 0.5 mM sulfuric acid and its flow rate, 0.5 mL min⁻¹. Under these conditions, the retention times were: 13.0 (formic acid), 15.2 (acetic acid) and 17.8 (propionic acid) minutes. The suppressor was regenerated with 30 mM lithium chloride solution.

The concentration of the formed aldehydes (formaldehyde, acetaldehyde and propionaldehyde) was determined by HPLC-DAD. To that end, derivatization of the aldehydes with 2,4-dinitrophenylhydrazine (2,4-DNPH) to 2,4-dinitrophenylhydrazones was used [30]. Practically, a solution resulted by adding 0.2 mL 2,4-dinitrophenylhydrazine in acetonitrile (6 mM) and 0.1 mL perchloric acid in acetonitrile (1 M) to 1.7 mL sample, which was kept in dark for 45 min, was injected in a Shimadzu LC 20 chromatograph (Shimadzu Europa GmbH, Duisburg, Germany). The separation of hydrazones was carried out by using a C18 (NC-04, 250 mm × 4.0 mm ID, 5.0 μm, Prontosil) column (Bischoff Analysentechnik und Geräte GmbH, Leonberg, Germany). The eluent was acetonitrile in water (35%—2 min, 45%—3 min, 100%—20 min and 35%—15 min) at a flow rate of 0.5 mL min⁻¹. The retention times and wavelengths used for detection were 18.0 min/350 nm for formaldehyde, 18.8 min/359 nm for acetaldehyde and 19.7 min/360 nm for propionaldehyde. Under the above-mentioned conditions, the derivatization was considered as a quantitative process.

Formaldehyde was also determined spectrophotometrically by using the Hantzsch method. This is based on the reaction among formaldehyde, acetylacetone and ammonium acetate, when the product is a yellow compound that has an absorption maximum at 412 nm of $\epsilon(412) = 7700 \text{ M}^{-1} \text{ cm}^{-1}$ [31]. The technique consists of adding 2 mL Hantzsch reagent (25 g ammonium acetate, 3 mL glacial acetic acid and 0.2 mL acetylacetone brought to 100 mL with water) to 10 mL sample, keeping the obtained mixture for 30 min at 50 °C, and measuring the absorbance of the suddenly cooled sample against a blank.

The assessment of hydroxyl radical formation yield with respect to ozone was based on formaldehyde formation following the reaction between *tert*-butanol (acting as a scavenger) and hydroxyl radicals in the presence of oxygen [32]. For the systems where ozone occurs together with oxygen, Flyunt et al. have reported a 50% formaldehyde formation yield with respect to hydroxyl radicals [33].

Given that in our system formaldehyde also resulted following the reaction of 1-propanol with hydroxyl radicals, the calculation of hydroxyl radicals' formation yield with respect to ozone involves knowing formaldehyde formation yields with respect to ozone in the presence and absence of *tert*-butanol.

Formaldehyde formation yields in the two systems can be derived from the slopes of straight lines in the graphic representation of the formed formaldehyde concentration versus the introduced ozone concentration. An aspect that had to be taken into consideration with this method was the fact that usually isobutene may be present as impurity in *tert*-butanol, which could lead to formaldehyde following the reaction with ozone: $(\text{H}_3\text{C})_2\text{C}=\text{CH}_2 + \text{O}_3 + \text{H}_2\text{O} \rightarrow (\text{H}_3\text{C})_2\text{C}=\text{O} + \text{H}_2\text{C}=\text{O} + \text{H}_2\text{O}_2$ [34,35]. Given the fact that this reaction was fast, formaldehyde formed at the beginning and thus it did not exert influence on the slopes, but only on the y-intercepts.

Hydrogen peroxide quantification was carried out by using Allen's method [36]. This was based on the reaction between compounds such as R-O-O-H (R can be an H atom or an organic group) and I⁻, in excess, whereby I₃⁻ is formed. Given that this is usually a slow reaction, a catalyst, namely ammonium heptamolybdate, is introduced in the system. In the case of H₂O₂, the catalyst led to the increase of reaction rate constant from $1.8 \times 10^{-3} \text{ M}^{-1} \text{ s}^{-1}$ [33] to $2.1 \text{ M}^{-1} \text{ s}^{-1}$ [34]. Practically, 1 mL Allen's A (1 g NaOH, 33 g KI and 0.1 g (NH₄)₆Mo₇O₂₄·4H₂O dissolved in Millipore water and brought to 500 mL), 1 mL Allen's B (10 g potassium hydrogen phthalate dissolved in Millipore water and brought to 500 mL) and 1 mL sample were mixed in a 1 cm cuvette (in between additions the cuvette was strongly stirred). The absorbance of the mixture was read at 350 nm against a blank. The molar absorption coefficient of I₃⁻ was $\epsilon(350) = 25500 \text{ M}^{-1} \text{ cm}^{-1}$ [36].

Quantum chemical calculations were done by using the Density Functional Theory method (DFT) B3LYP [37,38], as implemented in Jaguar program [39]. The structures of the studied molecules were

optimized in water with Jaguar's Poisson-Boltzmann solver (PBF) [40] at B3LYP/6-311+G(d,p)/PBF level of theory. The frequency analysis was carried out to characterize the stationary points on the potential surface and to obtain Gibbs energy (G) at 298 K. The Gibbs energy of reactions (ΔG) were derived from the calculated Gibbs energies of reactants and products. The calculated Gibbs energies give some insight in the feasibility of the reactions. Actually the competition of pathways and product formation are determined by kinetics (for thermodynamically feasible reactions). Calculations of charged species as required for the Gibbs energy of equilibrium are inherently poorer. It was shown [23], that via B3LYP/6-311+G(d,p)/PBF method values comes closest to the experimental ones.

5. Conclusions

This study confirms the supposition that ozone reacts with 1-propanol in aqueous media mainly by hydride transfer as expected based on the results for 2-propanol/ozone aqueous system. In contrast to 2-propanol/ozone system, where insertion and H-abstraction have a share of a small percentage, ozone reacts with 1-propanol with yields of one order of magnitude higher as part of the afore-mentioned mechanisms. This is an important finding that linked to the fact that the nature of products depends on mechanism. Thus, the hydride transfer leads to aldehyde and ketone with the same number of carbon atoms as alcohols, while by insertion and H-abstraction, the result is a mix of acids and carbonyl compounds. This means that the same ozone consumption lead to a higher degree of oxidation and to fragmentation of the initial molecule for insertion and H-abstraction (other oxidants such as HO•, HO₂• and H₂O₂ are also formed). In addition, one can notice that the reaction rate between 1-propanol and ozone is four times lower than that between 2-propanol and ozone. The two second order rate constants are: $(6.4 \pm 0.2) \times 10^{-1} \text{ M}^{-1} \text{ s}^{-1}$ for 1-propanol and $(2.7 \pm 0.1) \text{ M}^{-1} \text{ s}^{-1}$ for 2-propanol. This finding is also correlated with the share of mechanisms.

The comparison between the 2-propanol/ozone and 1-propanol/ozone aqueous systems clearly shows that a small change in the structure of the molecule (in our case switching from a secondary alcohol to a primary one with the same number of carbon atoms) leads to significant variations in the nature and share of the reaction products and also on the reaction rate. This has a great impact, for example, in the treatment of waters. In this context, one may foresee that the water treatment will rely less on the use of some overall parameters and that it will be more and more specific, based on the knowledge of the exact composition of certain waters and the interaction with various chemicals used for water treatment.

Supplementary Materials: Supplementary materials can be found at <http://www.mdpi.com/1422-0067/20/17/4165/s1>.

Author Contributions: Conceptualization, E.R.; Investigation, E.R. and A.T.-R.; Resources, W.S. and T.C.S.; Software, S.N.; Visualization, E.R. and A.T.-R.; Writing—original draft, E.R.; Writing—review & editing, A.T.-R., S.N., W.S. and T.C.S.

Funding: This research received no external funding.

Acknowledgments: The authors thank Alexandra Fischbacher, Sarah Willach and Laura Wiegand of Universität Duisburg Essen; George A. Crisia of Aquatim S.A. Timișoara and Jens Richter of Westfälische Hochschule Gelsenkirchen for their kind help.

Conflicts of Interest: The authors declare no conflict of interest.

References

1. Hoigné, J.; Bader, H. Rate constants of reactions of ozone with organic and inorganic compounds in water—I. Non-dissociating organic compounds. *Water Res.* **1983**, *17*, 173–183. [[CrossRef](#)]
2. Willson, R.L.; Greenstock, C.L.; Adams, G.E.; Wageman, R.; Dorfman, L.M. The standardization of hydroxyl radical rate data from radiation chemistry. *Int. J. Radiat. Phys. Chem.* **1971**, *3*, 211–220. [[CrossRef](#)]
3. Adams, G.E.; Boag, J.W.; Michael, B.D. Reactions of the hydroxyl radical. Part 2. Determination of absolute rate constants. *Trans. Faraday Soc.* **1965**, *61*, 1417–1424. [[CrossRef](#)]

4. Neta, P.; Schuler, R.H. Rate constants for the reaction of $O\bullet^-$ radicals with organic substrates in aqueous solution. *J. Phys. Chem.* **1975**, *79*, 1–6. [[CrossRef](#)]
5. Reisz, E.; von Sonntag, C.; Tekle-Röttering, A.; Naumov, S.; Schmidt, W.; Schmidt, T.C. Reaction of 2-propanol with ozone in aqueous media. *Water Res.* **2018**, *128*, 171–182. [[CrossRef](#)] [[PubMed](#)]
6. Reisz, E.; Fischbacher, A.; Naumov, S.; von Sonntag, C.; Schmidt, T.C. Hydride transfer: A dominating reaction of ozone with tertiary butanol and formate ion in aqueous solution. *Ozone Sci. Eng.* **2014**, *36*, 532–539. [[CrossRef](#)]
7. Von Sonntag, C.; von Gunten, U. *Chemistry of Ozone in Water and Wastewater Treatment: From Basic Principles to Applications*; International Water Association Publishing: London, UK, 2012.
8. Plesnicar, B.; Cerkovnik, J.; Tekavec, T.; Koller, J. On the mechanism of the ozonation of isopropyl alcohol: An experimental and density functional theoretical investigation. ^{17}O NMR spectra of hydrogen trioxide (HOOOH) and the hydrotrioxide of isopropyl alcohol. *J. Am. Chem. Soc.* **1998**, *120*, 8005–8006. [[CrossRef](#)]
9. Plesnicar, B.; Cerkovnik, J.; Tekavec, T.; Koller, J. ^{17}O NMR spectroscopic characterisation and the mechanism of formation of alkyl hydrotrioxides (ROOOH) and hydrogen trioxide (HOOOH) in the low-temperature ozonation of isopropyl alcohol and isopropyl methyl ether: Water-assisted decomposition. *Chem. Eur. J.* **2000**, *6*, 809–819. [[CrossRef](#)]
10. Rakovsky, S.K.; Anachkov, M.; Zaikov, G.E.; Stoyanov, O.V.; Sofina, S.Y. Reactions of ozone with alcohols, ketons, ethers and hydroxybenzenes. Part 1. *Vestn. Kazan. Tekhnol. Univ.* **2013**, *16*, 11–16.
11. Wolfenden, B.S.; Willson, R.L. Radical-cations as reference chromogens in kinetic studies of one-electron transfer reactions: Pulse radiolysis studies of 2,2'-azinobis-(3-ethylbenzthiazoline-6-sulphonate). *J. Chem. Soc. Perkin Trans.* **1982**, *2*, 805–812. [[CrossRef](#)]
12. Buxton, G.V.; Greenstock, C.L.; Helman, W.P.; Ross, A.B. Critical review of rate constants for reactions of hydrated electrons, hydrogen atoms and hydroxyl radicals ($HO\bullet/O\bullet^-$) in aqueous solution. *J. Phys. Chem. Ref. Data* **1988**, *17*, 513–886. [[CrossRef](#)]
13. Plesnicar, B. Progress in the chemistry of dihydrogen trioxide (HOOOH). *Acta Chim. Slov.* **2005**, *52*, 1–12.
14. Czapski, G.; Bielski, B.H.J. The formation and decay of H_2O_3 and HO_2 in electron-irradiated aqueous solutions. *J. Phys. Chem.* **1963**, *67*, 2180–2184. [[CrossRef](#)]
15. Bielski, B.H.J.; Schwarz, H.A. The absorption spectra and kinetics of hydrogen sesquioxide and the perhydroxyl radical. *J. Phys. Chem.* **1968**, *72*, 3836–3841. [[CrossRef](#)]
16. Bothe, E.; Behrens, G.; Schulte-Frohlinde, D. Mechanism of the first order decay of 2-hydroxy-propyl-2-peroxyl radicals and of $O_2\bullet^-$ formation in aqueous solution. *Z. Naturforsch.* **1977**, *32*, 886–889. [[CrossRef](#)]
17. Bothe, E.; Schulte-Frohlinde, D. The bimolecular decay of the α -hydroxymethylperoxyl radicals in aqueous solution. *Z. Naturforsch.* **1978**, *33*, 786–788. [[CrossRef](#)]
18. Bothe, E.; Schuchmann, M.N.; Schulte-Frohlinde, D.; von Sonntag, C. Hydroxyl radical-induced oxidation of ethanol in oxygenated aqueous solutions. A pulse radiolysis and product study. *Z. Naturforsch.* **1983**, *38*, 212–219. [[CrossRef](#)]
19. Von Sonntag, C.; Schuchmann, H.-P. Peroxyl radicals in aqueous solutions. In *Peroxyl Radicals*; Alfassi, Z.B., Ed.; John Wiley & Sons Ltd.: Chichester, UK, 1997; pp. 173–234.
20. Bielski, B.H.J.; Cabelli, D.E.; Arudi, R.L.; Ross, A.B. Reactivity of HO_2/O_2^- radicals in aqueous solution. *J. Phys. Chem. Ref. Data* **1985**, *14*, 1041–1100. [[CrossRef](#)]
21. Russel, G.A. Deuterium-isotope effects in the autoxidation of aralkyl hydrocarbons. Mechanism of the interaction of peroxyl radicals. *J. Am. Chem. Soc.* **1957**, *79*, 3871–3877. [[CrossRef](#)]
22. Bennett, J.E.; Summers, R. Product studies of the mutual termination reactions of sec-alkylperoxy radicals: Evidence for non-cyclic termination. *Can. J. Chem.* **1974**, *52*, 1377–1379. [[CrossRef](#)]
23. Naumov, S.; von Sonntag, C. The reaction $HO\bullet$ with O_2 , the decay of $O_3\bullet^-$ and the pKa of $HO_3\bullet$ —Interrelated questions in aqueous free-radical chemistry. *J. Phys. Org. Chem.* **2011**, *24*, 600–602. [[CrossRef](#)]
24. Sein, M.M.; Golloch, A.; Schmidt, T.C.; von Sonntag, C. No marked kinetic isotope effect in the peroxone ($H_2O_2/D_2O_2 + O_3$) reaction: Mechanistic consequences. *ChemPhysChem* **2007**, *8*, 2065–2067. [[CrossRef](#)]
25. Merényi, G.; Lind, J.; Naumov, S.; von Sonntag, C. Reaction of ozone with hydrogen peroxide (peroxone process): A revision of current mechanistic concepts based on thermokinetic and quantum-chemical considerations. *Environ. Sci. Technol.* **2010**, *44*, 3505–3507. [[CrossRef](#)]

26. Merényi, G.; Lind, J.; Naumov, S.; von Sonntag, C. The reaction of ozone with the hydroxide ion: Mechanistic considerations based on thermokinetic and quantum chemical calculations and the role of HO_4^- in superoxide dismutation. *Chem. Eur. J.* **2010**, *16*, 1372–1377. [[CrossRef](#)]
27. Elliot, A.J.; McCracken, D.R. Effect of temperature on $\text{O}_2^{\bullet-}$ reactions and equilibria: A pulse radiolysis study. *Radiat. Phys. Chem.* **1989**, *33*, 69–74.
28. Thomas, J.K. Rates of reaction of the hydroxyl radical. *Trans. Faraday Soc.* **1965**, *61*, 702–707. [[CrossRef](#)]
29. Asmus, K.-D.; Möckel, H.; Henglein, A. Pulse radiolytic study of the site of HO^\bullet radical attack on aliphatic alcohols in aqueous solution. *J. Phys. Chem.* **1973**, *77*, 1218–1221. [[CrossRef](#)]
30. Lipari, F.; Swarin, S.J. Determination of formaldehyde and other aldehydes in automobile exhaust with an improved 2,4-dinitrophenyl-hydrazine method. *J. Chrom.* **1982**, *247*, 297–306. [[CrossRef](#)]
31. Nash, T. The colorimetric estimation of formaldehyde by means of the Hantzsch reaction. *Biochem. J.* **1953**, *55*, 416–421. [[CrossRef](#)]
32. Schuchmann, M.N.; von Sonntag, C. Hydroxyl radical-induced oxidation of 2-methyl-2-propanol in oxygenated aqueous solution. A product and pulse radiolysis study. *J. Phys. Chem.* **1979**, *83*, 780–784. [[CrossRef](#)]
33. Flyunt, R.; Leitzke, A.; Mark, G.; Mvula, E.; Reisz, E.; Schick, R.; von Sonntag, C. Determination of HO^\bullet , $\text{O}_2^{\bullet-}$, and hydroperoxide yields in ozone reactions in aqueous solution. *J. Phys. Chem. B* **2003**, *107*, 7242–7253. [[CrossRef](#)]
34. Dowideit, P.; von Sonntag, C. Reaction of ozone with ethene and its methyl- and chlorine-substituted derivatives in aqueous solution. *Environ. Sci. Technol.* **1998**, *32*, 1112–1119. [[CrossRef](#)]
35. Sängler, D.; von Sonntag, C. UV-photolysis ($\lambda = 185 \text{ nm}$) of liquid t-butanol. *Tetrahedron* **1970**, *26*, 5489–5501. [[CrossRef](#)]
36. Allen, A.O.; Hochanadel, C.J.; Ghormley, J.A.; Davis, T.W. Decomposition of water and aqueous solutions under mixed fast neutron and gamma radiation. *J. Phys. Chem.* **1952**, *56*, 575–586. [[CrossRef](#)]
37. Becke, A.D. Density-functional thermochemistry. III. The role of exact exchange. *J. Chem. Phys.* **1993**, *98*, 5648–5652. [[CrossRef](#)]
38. Lee, C.; Yang, W.; Parr, R.G. Development of the Colle-Salvetti correlation-energy formula into a functional of the electron density. *Phys. Rev. B* **1988**, *37*, 785–789. [[CrossRef](#)]
39. Jaguar 9.6; Schrodinger Inc.: New York, NY, USA, 2017.
40. Tannor, D.J.; Marten, B.; Murphy, R.; Friesner, R.A.; Sitkoff, D.; Nicholls, A.; Ringnalda, M.; Goddard, W.A.; Honig, B. Accurate first principles calculation of molecular charge distributions and solvation energies from ab initio quantum mechanics and continuum dielectric theory. *J. Am. Chem. Soc.* **1994**, *116*, 11875–11882. [[CrossRef](#)]



© 2019 by the authors. Licensee MDPI, Basel, Switzerland. This article is an open access article distributed under the terms and conditions of the Creative Commons Attribution (CC BY) license (<http://creativecommons.org/licenses/by/4.0/>).